Biochem. J. (2012) **448**, 141–152 (Printed in Great Britain) doi:10.1042/BJ20121008

Calpain-1 knockout reveals broad effects on erythrocyte deformability and physiology

Adam WIESCHHAUS*†‡, Anwar KHAN‡, Asma ZAIDI§, Henry ROGALIN*, Toshihiko HANADA*, Fei LIU‖, Lucia DE FRANCESCHI¶, Carlo BRUGNARA**, Alicia RIVERA** and Athar H. CHISHTI*†[1]

*Department of Molecular Physiology and Pharmacology, Tufts University School of Medicine, Boston, MA 02111, U.S.A., †Sackler School of Graduate Biomedical Sciences, Programs in Physiology, Pharmacology, and Microbiology, Tufts University, Boston, MA 02111, U.S.A., ‡Department of Pharmacology, University of Illinois College of Medicine, Chicago, IL 60612, U.S.A., §Department of Biochemistry, Kansas City University of Medicine and Biosciences, Kansas City, MO 64106, U.S.A., ‖Molecular and Integrative Physiological Sciences, Department of Environmental Health, Harvard School of Public Health, Boston, MA 02115, U.S.A., ¶Department of Medicine, University of Verona, Piazzale L.A. Scuro 10, Verona 37134, Italy, and **Department of Laboratory Medicine, Boston Children's Hospital, Harvard Medical School, Boston, MA 02115, U.S.A.

Pharmacological inhibitors of cysteine proteases have provided useful insights into the regulation of calpain activity in erythrocytes. However, the precise biological function of calpain activity in erythrocytes remains poorly understood. Erythrocytes express calpain-1, an isoform regulated by calpastatin, the endogenous inhibitor of calpains. In the present study, we investigated the function of calpain-1 in mature erythrocytes using our calpain-1-null [KO (knockout)] mouse model. The calpain-1 gene deletion results in improved erythrocyte deformability without any measurable effect on erythrocyte lifespan *in vivo*. The calcium-induced sphero-echinocyte shape transition is compromised in the KO erythrocytes. Erythrocyte membrane proteins ankyrin, band 3, protein 4.1R, adducin and dematin are degraded in the calcium-loaded normal erythrocytes but not in the KO erythrocytes. In contrast, the integrity of spectrin and its state of phosphorylation are not affected in the calcium-loaded erythrocytes of either genotype. To assess the functional consequences of attenuated cytoskeletal remodelling in the KO erythrocytes, the activity of major membrane transporters was measured. The activity of the K^+–Cl^- co-transporter and the Gardos channel was significantly reduced in the KO erythrocytes. Similarly, the basal activity of the calcium pump was reduced in the absence of calmodulin in the KO erythrocyte membrane. Interestingly, the calmodulin-stimulated calcium pump activity was significantly elevated in the KO erythrocytes, implying a wider range of pump regulation by calcium and calmodulin. Taken together, and with the atomic force microscopy of the skeletal network, the results of the present study provide the first evidence for the physiological function of calpain-1 in erythrocytes with therapeutic implications for calcium imbalance pathologies such as sickle cell disease.

Key words: calcium pump, calpain-1, deformability, erythrocyte, K^+–Cl^- co-transporter (KCC1), spectrin.

INTRODUCTION

Calpains are widely expressed cysteine proteases activated by calcium at neutral pH. They play functional roles in numerous physiological processes, including cytoskeletal reorganization, cell motility, apoptosis, neuronal biogenesis and haemostasis [1,2]. Genome sequencing has identified at least 14 members of the calpain superfamily. Among them, calpain-1 and calpain-2, also designated as μ-calpain and m-calpain respectively, remain the two most well-characterized members of the calpain family of proteases. Calpain-1, encoded by the *Capn1* gene, requires lower calcium concentration for activation, whereas calpain-2, encoded by the *Capn2* gene, is activated at higher concentrations of calcium [1]. A delicate balance exists *in vivo* between calpain-1, calpain-2 and calpastatin, the endogenous inhibitor of both calpains, providing a regulatory mechanism for calcium-mediated activation of calpain activity. Both calpain-1 and calpain-2 are expressed in varying levels in most mammalian tissues [3]. In general, the expression of calpain-1 dominates in the haematopoietic compartment, whereas calpain-2 expression is more prominent in the nonhaemopoietic cells. Since pharmacological inhibitors generally cannot distinguish between calpain-1 and calpain-2 activity, and may exert off-target effects, gene targeting has been employed to tease out the specific function of calpains *in vivo*.

The erythrocyte has served as a useful model system to study the physiological role of calpain activity in mammalian cells. The rationale for this approach was based on the expectation that identification of calpain-1 substrates in erythrocytes may provide leads for calpain-1 function in other cell types, since homologues of erythrocyte proteins exist in many non-erythroid cells. The mature erythrocyte offers a unique model system where calpain-1 function can be evaluated in the absence of calpain-2 activity [3,4]. Moreover, mature erythrocytes lack any internal calcium storage organelles, thus permitting assessment of calpain-1 function mostly at the plasma membrane. For example, previous studies have shown calpain-mediated cleavage of membrane-bound Ca^{2+}-ATPase, also known as calcium pump or PMCA (plasma-membrane Ca^{2+}-ATPase), which regulates calcium transport in erythrocytes [5,6]. Similarly, calpain-mediated proteolysis of haemoglobin is believed to provide a mechanism for the autocatalytic inactivation of calpain activity and formation of Heinz bodies. Activation of calpain is also required for the regulation of erythrocyte membrane fusion events triggered by the influx of calcium [7]. Moreover, evidence suggests that calpain activity plays a role in the regulation of protein phosphorylation

Abbreviations used: AFM, atomic force microscopy; CaM, calmodulin; CWS, choline wash solution; EI, elongation index; KCC1, K^+–Cl^- co-transporter; KO, knockout; MCV, mean cell volume; NHS, *N*-hydroxysuccinimide; PKC, protein kinase C; PKM, protein kinase M; PMCA, plasma-membrane Ca^{2+}-ATPase; PVP, polyvinylpyrrolidone; WT, wild-type.

[1] To whom correspondence should be addressed (email athar.chishti@tufts.edu).

of erythrocyte membrane proteins such as protein 4.1R [8]. Since phosphorylation of protein 4.1R modulates its interaction with spectrin, actin and the plasma membrane, it was proposed that calpain-mediated proteolysis of PKC (protein kinase C), which phosphorylates protein 4.1R, is required for erythrocyte survival during circulatory stress *in vivo* [8].

The functional role of calpain activity in erythrocytes has been traditionally investigated by employing the pharmacological inhibitors of cysteine proteases [8]. For example, the role of calpain activity in the regulation of erythrocyte PKC was established by resealing the calpain inhibitors leupeptin and E-64 in mature erythrocytes [8]. Although this approach has been successful in inhibiting calpain activity in erythrocytes, the possibility of off-target effects by these synthetic inhibitors cannot be ruled out. A case in point is calpeptin, a known calpain inhibitor that also inhibits the calpeptin-sensitive protein-tyrosine phosphatase acting upstream of the RhoA GTPase [9]. To overcome these limitations, we used calpain-1-null mice to investigate the effect of calpain-1 loss in mature erythrocytes in the absence of compensation by either calpain-2 or any other cysteine protease. We provide the first evidence that calpain-1 negatively regulates erythrocyte deformability and filterability without any discernible effect on erythrocyte lifespan under normal conditions. Our findings also reveal some unexpected consequences of calpain-1 loss on erythrocyte shape, activity of transporters and phosphorylation of membrane proteins. Together, these results raise the possibility that selective pharmacological inhibition of calpain-1 may offer new therapeutic options for erythrocyte pathologies with aberrant calcium homoeostasis, such as sickle cell disease.

EXPERIMENTAL

Antibodies and reagents

Antibodies against spectrin, ankyrin, band 3, protein 4.1R, dematin and p55 were generated in our laboratory. A monoclonal antibody against calpain was purchased from NOVACASTRA, and a monoclonal antibody (5F10) against the erythrocyte calcium pump (PMCA) was a gift from Dr Emanuel Strehler (Mayo Clinic, Rochester, MN, U.S.A.). The calcium ionophore A23187 was purchased from Calbiochem. [^{32}P]P_i was obtained from DuPont New England Nuclear. PMA, DMSO, dibutyryl-cAMP and other common reagents were purchased from Sigma.

Haematological analysis

Mice were anaesthetized by inhalation of 3 % isoflurane under an approved Institutional Animal Care and Use Committee protocol. Blood from 3–4-month-old WT (wild-type) and calpain-1 (*Capn1*)-null mice was collected in either heparin- or EDTA-containing tubes. Blood smears were stained with Wright-Giemsa (Sigma), and reticulocytes were counted after staining with New Methylene Blue (manual count). Erythrocyte and reticulocyte numbers were determined using an automated haematological analyser (ADVIA 120; Multispecies software; Siemens Diagnostic Solutions).

Erythrocyte deformability

Blood was collected into acid citrate dextrose anticoagulant and used within 24 h. Blood ($\sim$850 μl) was drawn from mice via the inferior vena cava while anaesthetized using isoflurane, transferred to 1.5 ml tubes, and spun at 1000 ***g*** for 5 min. After removing plasma and buffy coat by aspiration, erythrocytes were washed with PBS and spun again at 1000 ***g*** for 5 min. Erythrocytes were then transferred to 15 ml tubes and washed twice using PBS and centrifugation at 1500 ***g*** for 5 min. Erythrocytes were suspended in 1.0 ml of calcium-free Tyrode's buffer (10 mM Hepes, 12 mM $NaHCO_3$, pH 7.5, 137 mM NaCl, 2.5 mM KCl, 5 mM glucose and 0.1 % BSA), and counted using a haemocytometer. Samples were normalized to 8×10^6 cells/mm^3 with Tyrode's buffer. Experimental samples were prepared using 200 μl of erythrocyte suspension and 800 μl of Tyrode's buffer with A23187 added to a final concentration of 1.0 μM, with and without 50 μM calcium. The erythrocytes were incubated at 37 °C for 20 min, spun down at 1000 ***g*** for 5 min, and suspended in 100 μl of Tyrode's buffer.

Erythrocyte deformability was assessed using a laser diffraction Ektacytometer with a thin micro-channel as the shearing geometry (RheoScan-D300; RheoMeditech) [10,11]. The erythrocyte suspension (6 μl) of each genotype was mixed with the PBS-PVP (polyvinylpyrrolidone) aliquot (600 μl volume). The PBS-PVP solution was provided as part of the commercial kit with the RheoScan-D300 instrument. The erythrocyte mixture (500 μl) was transferred to the cartridge and tested using RheoScan-D300. Each sample was tested at least three times each in this manner. The RheoScan-D300 measures the length and width of the erythrocytes at 16 shear stress levels from 20 to 0.5 Pa using a CCD (charge-coupled-device) camera and computer to measure the EI (elongation index). The EI is calculated as EI = (L − W)/(L + W), and the results are given as means ± S.D. in the Figures.

Erythrocyte filterability

Analysis of the rate of filtration of an erythrocyte suspension through a highly uniform nickel mesh filter was conducted by a gravity-based vertical tube method as described in [12]. This method measures the rate of passage of erythrocytes through the filter as a function of hydrostatic pressure (Tsukusa Sokken). The pore diameter of the nickel mesh used in the present study was 4.6 μm. From a height (pressure)–time curve obtained during the filtration analysis, a pressure–flow rate relationship can be determined. The filtration was started at a pressure of 150 mmH_2O, and the percentage of the flow rate (ml/min) of the erythrocyte suspension (0.1 % haematocrit) in Hepes buffer (96 mM KCl, 64 mM NaCl, 10 mM glucose, 1.0 mM $MgCl_2$ and 16 mM Hepes, pH 7.5) relative to that of the aqueous suspending medium at 100 mmH_2O was taken as the index of erythrocyte filterability.

Erythrocyte osmotic fragility

Osmotic fragility assay was performed on freshly obtained erythrocytes from 4–6-month-old WT and calpain-1-null mice in the presence of heparin as an anticoagulant. Blood was washed three times with PBS and resuspended in PBS at 20 % haematocrit, followed by incubation with either 1.0 μM of the calcium ionophore A23187, or 1.0 μM A23187 plus 100 μM $CaCl_2$ for 15 min at 37 °C. Erythrocytes were washed twice with the ice-cold salt solution (154 mM NaCl, 9.5 mM Na_2HPO_4 and 1.5 mM NaH_2PO_4, pH 7.4; 100 % salt solution) to terminate calcium loading. Erythrocyte lysis was monitored by the release of haemoglobin into the supernatant upon incubation of cells with graded salt concentrations (100–1 %) for 30 min at room temperature (23 °C). Erythrocyte suspensions were centrifuged and the absorbance of the supernatant was recorded at 540 nm. Each sample in water was taken as 100 % erythrocyte lysis, and readings of the same sample in various osmolarity solutions were normalized.

Erythrocyte lifespan

The *in vivo* lifespan of erythrocytes was determined as described previously [13]. Briefly, adult mice were injected with NHS (*N*-hydroxysuccinimide)–biotin through a tail-vein injection. Blood was drawn in PBS-G (PBS plus 10 mM glucose) on specific days, and washed erythrocytes were incubated with avidin–FITC at 37 °C for 1 h. Erythrocytes were washed with PBS-G, and the percentage of labelled cells was determined by flow cytometry. Erythrocyte labelling was greater than 95 %, and in most experiments, the labelling was close to 99 %. The same gate was used for both WT and calpain-1-null erythrocytes.

Erythrocyte shape change analysis

The erythrocyte shape change assay was performed essentially as described previously [14]. Briefly, blood from six WT and six calpain-1-null mice was drawn into a syringe containing 3.8 % trisodium citrate (1:10, v/v). Blood pooled from each genotype was centrifuged at 100 ***g*** for 10 min. The erythrocyte pellet was washed three times and resuspended in HBSS (Hanks buffered salt solution, pH 7.3) containing 0.1 % BSA but devoid of calcium. A final spin of 800 ***g*** for 10 min was performed to pack the erythrocytes, and the cells were resuspended in medium as described above to 1 % haematocrit. Each sample was incubated at 37 °C without calcium, and with 50 μM or 1.0 mM $CaCl_2$ in the presence of 1.5 μM calcium ionophore A23187 for up to 60 min. Erythrocyte samples were then placed on to a siliconized glass slide, and visualized by DIC (differential interference contrast) microscopy using a 100× objective on a Nikon Eclipse TE2000-E inverted microscope. A total of ten random fields of acquired images were analysed for quantification of erythrocyte morphology at different time intervals. The images are representative of three independent experiments.

SDS/PAGE and Western blotting

Erythrocyte membrane proteins from ghosts were separated on 8 % polyacrylamide gels and stained with Coomassie Blue (Laemmli gel system). Proteins were transferred on to a nitrocellulose membrane (Bio-Rad Laboratories), blocked with 5 % non-fat dried skimmed milk powder in Tris-buffered saline (BDH Chemicals) containing 0.1 % Tween 20, and analysed with the respective antibodies. Enhanced chemiluminescence detection was performed using the SuperSignal West Pico kit (Pierce).

Calpain-1 activation and erythrocyte membrane proteins

Blood was collected from WT and calpain-1-null mice in heparin tubes. Erythrocytes were washed with PBS to remove the buffy coat, and resuspended in calcium-free Tyrode's buffer. For activation of calpain-1, erythrocytes were incubated with 1.0 μM calcium ionophore A23187 for 3.0 min at 37 °C followed by the addition of various concentrations of $CaCl_2$. Erythrocytes were further incubated for 10–20 min at 37 °C, and incubation was terminated by cell lysis in 10 vol. of ice-cold lysis buffer (5 mM sodium phosphate buffer, pH 8.0, 1.0 mM EDTA and 1.0 mM PMSF). Erythrocyte ghosts were prepared, resuspended in SDS sample buffer, and analysed by SDS/PAGE and Western blotting.

Radioactive labelling of erythrocyte membrane proteins

Freshly harvested erythrocytes were resuspended at 20 % haematocrit in solution A (145 mM NaCl, 5.0 mM KCl, 10 mM Hepes, pH 7.4, and 0.1 mM Na_2HPO_4), and incubated at 37 °C with 0.4 mCi/ml of [^{32}P]P_i for 2 h to label the intracellular ATP pool. Aliquots (250 μl) of cells were then treated with either 2.0 mM dibutyryl-cAMP or 1.0 μM PMA, or 1.0 μM calcium ionophore A23187 plus 500 μM of $CaCl_2$ at 37 °C for the indicated time intervals. Erythrocytes were washed once with ice-cold solution A, and then immediately lysed with 10 vol. of ice-cold lysis buffer. Erythrocyte ghosts were washed twice with lysis buffer, solubilized in SDS sample buffer, and radiolabelled proteins were visualized by SDS/PAGE (8 % gels) and autoradiography.

Erythrocyte K^+–Cl^- co-transport activity

K^+–Cl^- co-transport and ion content

Heparinized blood collected from the mouse inferior vena cava was processed for measurement of red cell indices using an ADVIA 120 haemoanalyser (Siemens Diagnostic Solutions). Plasma and buffy coat were removed after passing through cotton, and cells were centrifuged at 1350 ***g*** for 4 min at 4 °C. The red cell pellet was washed four times with an ice-cold CWS (choline wash solution) containing 172 mM choline chloride, 1.0 mM $MgCl_2$ and 10 mM Tris/Mops, pH 7.4, at 4 °C as described previously [15]. An aliquot of cells was then suspended at 50 % volume with Mg^{2+}-free CWS, and determinations of haematocrit and cell Mg^{2+} (1:50 dilution) were performed. Erythrocyte Mg^{2+} content was determined by atomic absorption spectrophotometry with standards made in double distilled water. The activity of KCC1 (K^+–Cl^- co-transporter) was calculated as the difference between K^+ efflux in hypotonic NaCl (100 mM), isotonic NaCl (160 mM), and hypotonic sodium sulfamate (100 mM) media [16]. Fluxes were measured between 5 and 35 min at 37 °C, and the flux was estimated from the slope of the time course curve. The maximal rates of KCC1 activity was calculated from the difference between the volume-sensitive fraction and the Cl^--dependent K^+ flux, and expressed as mmol/10^{13} cells per h.

Gardos channel activity

Freshly washed erythrocytes were suspended at 2 % haematocrit in isotonic influx media containing 165 mM NaCl, 2.0 mM KCl, 0.15 mM $MgCl_2$, 1.0 mM ouabain and 10 mM Tris/Mops, pH 7.4, at 22 °C, 10 μM bumetanide and 10 μCi/ml ^{86}Rb in the presence or absence of 50 nM charybdotoxin, a specific blocker of the Gardos channel. Free Ca^{2+} in the influx media was buffered to 7.0 μM with 1.0 mM citrate buffer as described previously [15]. At zero time, calcium ionophore A23187 (5 μM) was added and aliquots were removed at 0.33, 2 and 5 min and immediately spun down through 0.8 ml of unlabelled medium containing 5.0 mM EGTA buffer and an underlying cushion of n-butyl phthalate. Supernatants were aspirated, and the tube tip containing the radioactive cell pellet was cut off. The erythrocyte-associated radioactivity was measured in a gamma counter (model 41 600 HE; Isomedic ICN-MP Biomedicals). The K^+ uptake was linear up to 5 min, and fluxes were calculated from the slope of the linear regression as described previously [15].

Erythrocyte calcium pump activity

Isolation of erythrocyte membranes

Mouse erythrocyte membranes were isolated from freshly collected blood as described previously [17]. Briefly, blood

was centrifuged at 1942 ***g*** for 15 min, plasma and buffy coat were aspirated off, and erythrocytes were lysed in a hypotonic buffer containing 10 mM Tris/HCl, pH 6.7, and 0.5 mM EDTA. Membranes (ghosts) were centrifuged several times at 10 000 rev./min for 20 min in a JA20 rotor to remove haemoglobin, and washed using a hypertonic buffer containing 10 mM Hepes, pH 7.2, 120 mM KCl, 0.5 mM $MgCl_2$ and 50 μM $CaCl_2$ until free of haemoglobin. Protein concentration was determined using a BCA (bicinchoninic acid) kit (Pierce). Ghosts were divided into small aliquots and frozen at $-80\,^{\circ}C$ until further analysis.

Measurement of PMCA activity

Erythrocyte membranes isolated from the WT and calpain-1-null mice were assayed for PMCA activity in a 96-well plate using the Malachite Green colorimetric assay [18]. Activity of PMCA was determined by measuring the release of P_i by calcium-dependent ATP hydrolysis. Each well, in a final volume of 100 μl, contained 25 mM Tris/HCl, pH 7.4, 50 mM KCl, 1.0 mM $MgCl_2$, 0.1 mM ouabain, 4.0 μg/ml oligomycin, 200 μM EGTA and $CaCl_2$ to give the desired final free Ca^{2+} concentration (ranging from 1–10 μM). The final free Ca^{2+} concentration was calculated using the software calcium.com, which calculates multiple equilibria between all ligands in solution. The PMCA activity, measured in the presence of calcium without CaM (calmodulin), is referred to as the 'basal' activity, and that measured in the presence of calcium and CaM (340 nM) as 'CaM-stimulated' activity. After a 5 min pre-incubation of PMCA with the assay components, the reaction was started by the addition of ATP (1.0 mM final concentration), continued for 30 min at 37 °C, and stopped by the addition of Malachite Green dye. The contents were made acidic by the addition of 19.5 % H_2SO_4, incubated for 45 min, and colour measured at 650 nm in a plate reader. The PMCA activity was defined as the calcium-activated ATP hydrolysis and expressed as nanomoles of P_i liberated per mg of protein per min based on the values from a standard curve of the absorbance at various concentrations of free P_i.

AFM (atomic force microscopy)

Erythrocyte attachment on the surface-modified glass coverslips, cytoskeleton exposure, AFM and image analysis were all performed as described previously [13,19,20].

RESULTS

Protease activity in calpain-1-null erythrocytes

We generated calpain-1-null mice by targeted mutagenesis of the *Capn1* gene [4]. Targeted deletion of eight amino acids (residues 153–160) was introduced within exon 4 of the *Capn1* gene, followed by the insertion of the gene-disrupting pGK-Neo cassette. The calpain-1-null mice were backcrossed more than 20 generations on a C57BL/6 genetic background. Erythrocytes isolated from adult mice were analysed for calpain activity. Erythrocytes, free of platelets and leucocytes, were assayed for total calpain activity by casein zymography. The calpain-1-null erythrocytes were deficient of any detectable protease activity by casein zymography (results not shown), consistent with our previous findings using PCR and casein zymography [4]. Similarly, purified erythrocyte membranes (ghosts) free of haemoglobin were also completely deficient of any calpain activity by casein zymography (results not shown). Since both erythrocyte calpains migrate at the same position on SDS/PAGE under reducing conditions, a monoclonal antibody that detects both calpain-1 and calpain-2 enzymes with equal efficiency was used. Western blotting did not detect any calpain-reactive band in the calpain-1-null ghosts (results not shown). These results demonstrate that no compensatory induction of calpain-2 occurs in the adult calpain-1-null erythrocytes. Our results also indicate that calpain-1 is the dominant cysteine protease in adult mouse erythrocytes, since no protease activity was detected against the denatured casein and erythrocyte membrane proteins as substrates under these conditions.

Calpain-1-mediated proteolysis of erythrocyte membrane proteins

Using synthetic inhibitors of calpain activity, several attempts have been made to identify the substrates of calpain-1 in erythrocyte ghosts [21,22]. These studies identified multiple substrates of calpain activity in erythrocyte ghosts, including spectrin [21]. Similarly, using our calpain-1-null mice on a mixed genetic background, we have shown that proteolysis of several erythrocyte membrane proteins, including ankyrin, adducin, band 3, protein 4.1R and dematin, is inhibited in the calpain-1-null erythrocytes [23]. To further investigate the effect of calpain-1 deficiency on spectrin proteolysis and phosphorylation, intact erythrocytes were loaded with calcium via the calcium ionophore A23187, and membrane proteins were analysed for degradation and phosphorylation (Figure 1). It is to be noted that erythrocytes were purposely loaded with high concentrations of calcium for two reasons: (i) unlike human erythrocytes, we found that the mouse erythrocyte membrane proteins were relatively resistant to calcium-induced degradation under these conditions; and (ii) we wanted to examine if other calcium-dependent proteases exist that might be activated at high calcium concentrations, thus compensating for calpain-1 loss in the calpain-1-null erythrocytes.

Since we did not detect any measurable proteolysis of membrane proteins in WT erythrocytes loaded with 400 μM calcium after 10 min of incubation at 37 °C (results reviewed but not shown), proteolysis of membrane proteins was examined in mouse erythrocytes loaded with 1.0 mM calcium (Figure 1A). No proteolysis of membrane proteins was observed in the calpain-1-null erythrocytes even at high calcium concentrations (Figure 1A). It is to be noted that a relatively small reduction ($\sim$15 %) of protein 4.1R in the calcium-treated KO (knockout) cells could be attributed to transglutaminase-mediated cross-linking of membrane proteins, which is independent of calpain-1 loss in erythrocytes [23]. These findings indicate that calcium-dependent protease activity is absent in the calpain-1-null erythrocytes under these conditions. Interestingly, no degradation of spectrin was observed in either WT or KO erythrocytes, even at high calcium concentrations (Figures 1A and 1B). This observation was confirmed by Western blotting using a polyclonal antibody against spectrin (Figure 1C). In contrast, similar blotting experiments confirmed ankyrin, adducin, band 3, protein 4.1R and dematin as calpain-1 substrates, whereas protein 4.2 and actin were not degraded under these conditions (results not shown).

It is well known that erythrocyte membrane proteins, including β-spectrin, are phosphorylated by multiple protein kinases in intact erythrocytes [24]. To examine the dependence of protein kinase activity on calpain-1, particularly on β-spectrin phosphorylation, intact erythrocytes were metabolically labelled with radiolabelled phosphate. Protein kinases were activated with dibutyryl-cAMP, an activator of PKA (cAMP-dependent protein kinase); PMA, an activator of PKC; and calcium (500 μM) plus calcium ionophore A23187 (1.0 μM), to activate calcium-dependent kinases as well as calpain-1. Radiolabelled erythrocytes were incubated for 30 min at 37 °C,

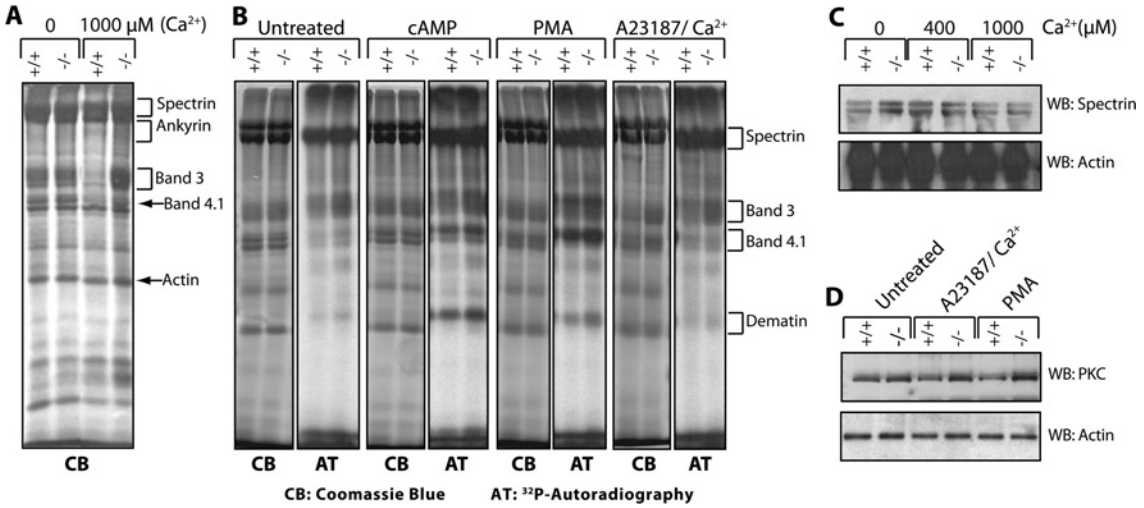

Figure 1 Proteolysis and phosphorylation of erythrocyte membrane proteins

(**A**) SDS/PAGE of erythrocyte ghosts [Coomassie Blue (CB): 50 μg of total protein] isolated from WT (+/+) and calpain-1-null (−/−) mice. Erythrocytes were treated with calcium ionophore A23187 (1.0 μM) and $CaCl_2$ (1.0 mM) at 37 °C for 10 min. The position of major membrane proteins is indicated. (**B**) SDS/PAGE of erythrocyte ghosts (50 μg of total protein) from WT (+/+) and calpain-1-null (−/−) mice. Intact erythrocytes were metabolically labelled with [^{32}P]P_i following stimulation with either 2.0 mM dibutyryl-cAMP or 1.0 μM PMA, or 1.0 μM A23187 plus 500 μM $CaCl_2$ for 30 min at 37 °C. The Coomassie Blue and autoradiogram (AT) panels of the same gel are shown. The position of major membrane proteins is indicated. (**C**) Western blot (WB) analysis of spectrin in WT (+/+) and calpain-1-null (−/−) ghosts at 400 and 1000 μM calcium. This analysis was performed since ankyrin migrates under the β-spectrin band, thus complicating the quantification of spectrin in the Coomassie-Blue-stained gels. No degradation of spectrin and p55/MPP1 was observed under these conditions. The lower panel shows the actin control for equal loading of the membrane proteins. (**D**) Western blot analysis of PKC proteolysis in ghosts isolated from WT (+/+) and calpain-1-null (−/−) erythrocytes following activation either with 1.0 μM PMA or 1.0 μM A23187 plus 500 μM $CaCl_2$. The lower panel shows the actin control for equal loading of the membrane proteins.

and phosphorylation of membrane proteins was examined by SDS/PAGE followed by autoradiography (Figure 1B). The loss of calpain-1 did not affect the phosphorylation of β-spectrin and other membrane proteins under these conditions (Figure 1B).

We noted that limited proteolysis of PKC occurred in the unstimulated, calcium-activated and PMA-stimulated WT erythrocytes, but not in the calpain-1-null erythrocytes (Figure 1D). This observation is consistent with previous evidence showing that PKC undergoes limited proteolysis by calpain to generate an active membrane-associated form designated as PKM (protein kinase M) [8,25]. The active PKM then phosphorylates membrane proteins, thus modulating the membrane properties in intact erythrocytes [24]. Surprisingly, all major phosphorylation targets, including β-spectrin, band 3, protein 4.1R and dematin, remained unaltered in the calpain-1-null erythrocytes (Figure 1B). These observations suggest that the conversion of PKC into PKM by calpain-1 is not required for regulating phosphorylation of major membrane proteins in mouse erythrocytes under these conditions.

Calpain-1 regulates erythrocyte shape change

On the basis of cysteine protease inhibitors, early evidence suggested that calpain activity plays a regulatory role in the transition of human erythrocyte shape from discocytes to echinocytes [26]. We investigated this observation using WT and calpain-1-null erythrocytes loaded with either low (50 μM) or high (1.0 mM) Ca^{2+} in the presence of calcium ionophore A23187 (1.5 μM). The erythrocyte shape, assessed by phase-contrast microscopy, showed normal discocyte morphology in both WT and KO erythrocytes under resting conditions (Figure 2). Calcium-loaded erythrocytes were incubated at 37 °C, and cell morphology was quantified at different time intervals (Figure 2). Calpain-1-null erythrocytes loaded with 50 μM calcium were significantly more susceptible to echinocyte and spheroechinocyte shape transition as compared with the WT erythrocytes over the 60 min incubation period (Figure 2A). When erythrocytes were exposed to high calcium concentrations, the echinocyte shape transition was again potentiated in the calpain-1-null erythrocytes for up to 15 min of incubation as compared with WT erythrocytes (Figure 2B, histogram). The number of echinocytes began to decrease in the calpain-1-null samples after 15 min of incubation with very few echinocytes detectable after 60 min of incubation at 37 °C (Figure 2B, histogram). Consistent with this observation, the number of spheroechinocytes significantly increased in the calpain-1-null samples upon calcium loading over the course of the 60 min incubation period (Figure 2, histograms). Together, these observations suggest that the loss of calpain-1 modulates the erythrocyte shape transition from discocyte to echinocyte/spheroechinocyte under these conditions.

Calpain-1 suppresses erythrocyte deformability and filterability

Since calpain-1 degrades key proteins of the erythrocyte membrane skeleton, it was of interest to determine whether loss of calpain-1 affects erythrocyte properties such as deformability and filterability. To investigate this possibility, WT and KO erythrocytes were incubated with calcium ionophore A23187 (1.0 μM) in calcium-free Tyrode's buffer and loaded with 50 μM calcium for 10 min at 37 °C. Erythrocytes were then subjected to increasing shear stress, and their deformability was measured using the Rheoscan-D300 Ektacytometer (Figure 3A). The maximum value of the deformability index, an approximate measure of the erythrocyte membrane deformability at the optimal surface to volume ratio, progressively increased with the shear stress (Figure 3A). Importantly, the deformability index was significantly higher in the calpain-1-null erythrocytes as compared with WT erythrocytes ($P < 0.02$ for all values shown in Figure 3A). As expected, the calcium loading caused a precipitous decline in the erythrocyte deformability of both

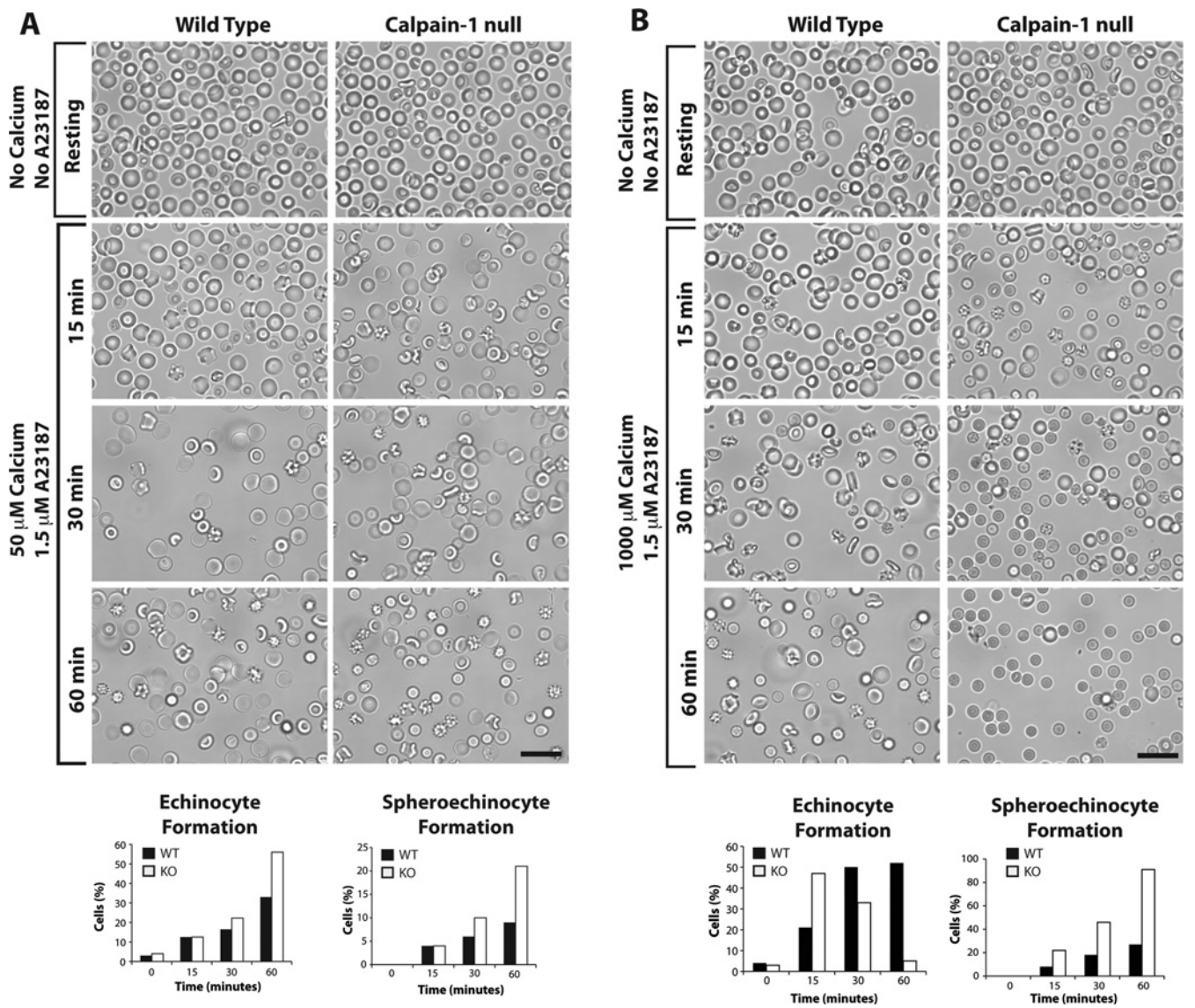

Figure 2 Calcium-induced erythrocyte shape change

(**A**) Erythrocytes from WT and calpain-1-null (KO) mice were treated with calcium ionophore A23187 (1.5 μM) and incubated with 50 μM $CaCl_2$. After incubation at 37 °C for specified time intervals, erythrocyte shape change was quantified by phase-contrast microscopy (bottom panels). (**B**) Same conditions as shown in (**A**), except the concentration of calcium was increased to 1000 μM. Note that the echinocyte formation was potentiated in the absence of calpain-1 at both calcium concentrations; however, the kinetics of echinocyte and spheroechinocyte formation was differentially regulated at higher calcium concentration. Scale bar, 10 μM.

genotypes (Figure 3A). Again, the deformability index was higher in the calpain-1-null erythrocytes as compared with the WT mice (Figure 3A).

To obtain a different measure of the impact of calpain-1 loss on erythrocyte rheology, we measured the filterability of the erythrocytes through a 4.6 μm nickel mesh (Figure 3B). The filtration rate of WT and KO erythrocytes was similar when both cell types were analysed in the absence of calcium loading (Figure 3B). However, following exposure to calcium ionophore A23187 and increasing concentrations of calcium for 30 min at 37 °C, the filtration rate of calpain-1-null erythrocytes was reproducibly higher as compared with WT erythrocytes (Figure 3B). For example, at 500 μM calcium, the mean filterability of the calpain-1-null erythrocytes was 18 % higher than the control erythrocytes, indicating that the absence of calpain-1 protects the cells against a calcium-induced decline in filtration rate. No erythrocyte lysis was observed under these conditions.

Effect of calpain-1 loss on erythrocyte fragility, density and lifespan

The effect of calcium influx on erythrocyte osmotic fragility was examined at different salt concentrations (Figures 4A and 4B). Washed erythrocytes treated with 1.0 μM calcium ionophore A23187 were loaded with 100 μM calcium for 15 min at 37 °C, and cell lysis was measured by haemoglobin release [13]. Although calcium influx into erythrocytes did shift the fragility curve in both genotypes, the statistical difference between the haemolysis of WT and KO erythrocytes was not significant (Figure 4A). However, in several osmotic fragility measurements, we noticed that the extent of haemolysis was slightly higher in the KO erythrocytes at a particular salt concentration. To investigate this observation further, we compared the haemolysis profile of freshly isolated erythrocytes with no exposure to ionophore and calcium (Figure 4B). This step was taken to potentially eliminate

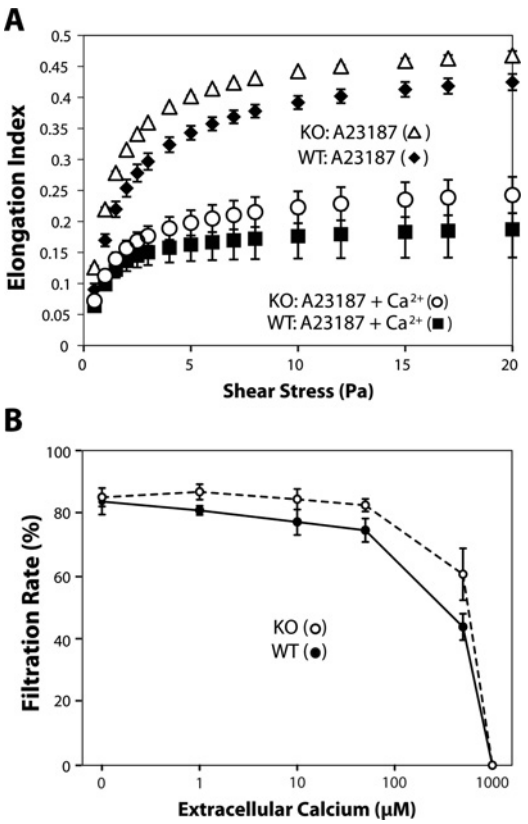

Figure 3 Erythrocyte deformability and filterability analysis

(**A**) Measurement of erythrocyte deformability by Ektacytometry. Erythrocytes from WT and KO mice were resuspended in calcium-free Tyrode's buffer, and treated with calcium ionophore A23187 (1.0 μM) and calcium (50 μM) as described in the Experimental section. Deformability measurements were performed in a RheoScan D-300 instrument. (**B**) Measurement of the erythrocyte filterability. WT and calpain-1-null (KO) erythrocytes were diluted to 0.1% haematocrit, and allowed to filter through a 4.6 μm pore nickel mesh filter. Data shown are means $\pm$ S.D. for four to six measurements from two independent experiments. Further details are given in the Experimental section.

the detrimental effects of the incubation period on erythrocyte properties. Overall, the haemolysis pattern was similar between the WT and KO erythrocytes at various salt concentrations (Figure 4B). However, we consistently noticed a small increase in the haemolysis of calpain-1-null erythrocytes at 200 m-osM salt concentration as compared with WT erythrocytes (Figure 4B).

Next, we measured the effect of calpain-1 loss on erythrocyte density using the oil-based microcapillary method as described previously [27]. There was a relatively small but reproducible shift towards the less dense and thus younger erythrocytes in the calpain-1-null mice (Figure 4C). Finally, the *in vivo* erythrocyte lifespan was determined by injecting NHS–biotin through the tail vein, and the percentage of biotin-labelled erythrocytes was measured by flow cytometry as described previously [13]. There was no significant difference in the *in vivo* half-life of calpain-1-null erythrocytes, as compared with WT mice, over the course of 50 days (Figure 4D).

K^+–Cl^- co-transport is deregulated in calpain-1-null erythrocytes

The increased deformability and filterability properties of calpain-1-null erythrocytes suggested potential deregulation in the cellular volume regulatory pathways. To investigate the possibility that calpain-1 gene deletion may induce changes in K^+ transport, we measured the activity of the Gardos channel and KCC1, both of which are known to play critical roles in the erythrocyte volume regulation. The activity of the Gardos channel was significantly reduced in the calpain-1-null erythrocytes as compared with WT mice (0.48 and 0.28 mmol/l cell per min respectively; $P < 0.03$, $n = 6$). Similarly, the KCC1 activity was also reduced in the calpain-1-null erythrocytes (WT $= 1.55 \pm 0.42$, KO $= 0.46 \pm 0.16$ mmol/10^{13} cell per h; $P < 0.04$, $n = 3$) (Figure 5A). These results suggest that the K^+ transport pathways are deregulated in the calpain-1-null erythrocytes under these conditions.

Calpain-1 differentially regulates erythrocyte calcium pump

Since the K^+ transport pathways are known to be activated by intracellular calcium, we surmised that the PMCA might be deregulated in the calpain-1-null erythrocytes. To test this possiblity, the PMCA activity was measured in the erythrocyte membranes (ghosts) over a range of free calcium concentrations (0–10 μM). The calcium pump activity was measured in the presence of inhibitors of known ATPases, thus ensuring the specificity of PMCA activity. The activity of the calcium pump was measured both in the absence and presence of exogenous CaM, a physiological regulator of the calcium pump [28]. The results indicated a linear increase in the pump activity with increasing calcium concentrations followed by a plateau (Figure 5B), consistent with earlier findings showing a Michaelis–Menten type of enzyme kinetics [29]. The addition of CaM to the PMCA assay resulted in the $\sim$2.5-fold stimulation of the basal pump activity (Figure 5B), attesting to the ability of this calcium sensor to serve as the physiological stimulator of PMCAs. There was a significant reduction in the V_{max} values of basal pump activity in the calpain-1-null ghosts as compared with the WT mice (Figure 5C). In contrast, the CaM-stimulated pump activity was relatively higher in the calpain-1-null ghosts as compared with the WT ghosts (Figure 5B). The reduction in basal activity and elevation in CaM-stimulated PMCA activity in calpain-1 KO erythrocytes (Figures 5B and 5C) suggest the possibility of the existence of a wider range of PMCA activity states in the calpain-1 KO mice, which in turn would allow greater variability in the levels of intracellular calcium levels in erythrocytes. The differential effect on PMCA activity was obvious from the V_{max} values shown in Figure 5(C), which were calculated from the curve fitting of the calcium curve data shown in Figure 5(B). The calculated V_{max} values in the WT and KO ghosts were 8.56 ± 0.31 and 4.07 ± 1.3 in the absence of CaM, and 20 ± 2.02 compared with 22.9 ± 0.9 in the presence of CaM respectively (Figure 5C). The difference in V_{max} values between WT and KO in the absence of CaM were statistically significant as determined by the Mann–Whitney Rank Sum Test ($P < 0.029$).

To investigate the basis of lower basal activity of PMCAs in the calpain-1-null ghosts (Figure 5C), the protein levels of both PMCA1 and PMCA4 isoforms, the two isoforms present in erythrocyte membranes, were examined by Western blotting. There were no detectable differences in the protein profile of PMCA isoforms between the WT and KO ghosts, suggesting that the observed reduction in the PMCA activity in KO ghosts is not mediated via altered PMCA protein levels, but may originate from differences in the regulation of enzyme activity. Nonetheless, we cannot rule out the possibility that subtle differences in the limited cleavage of erythrocyte PMCAs may have been missed by the Western blotting conditions used in the present study. Since the CaM-stimulated PMCA activity was elevated in the calpain-1-null ghosts (Figure 5C), a possibility exists that relatively less CaM may be associated with the calcium pump in calpain-1-null ghosts. To test this possibility, the amount of CaM was

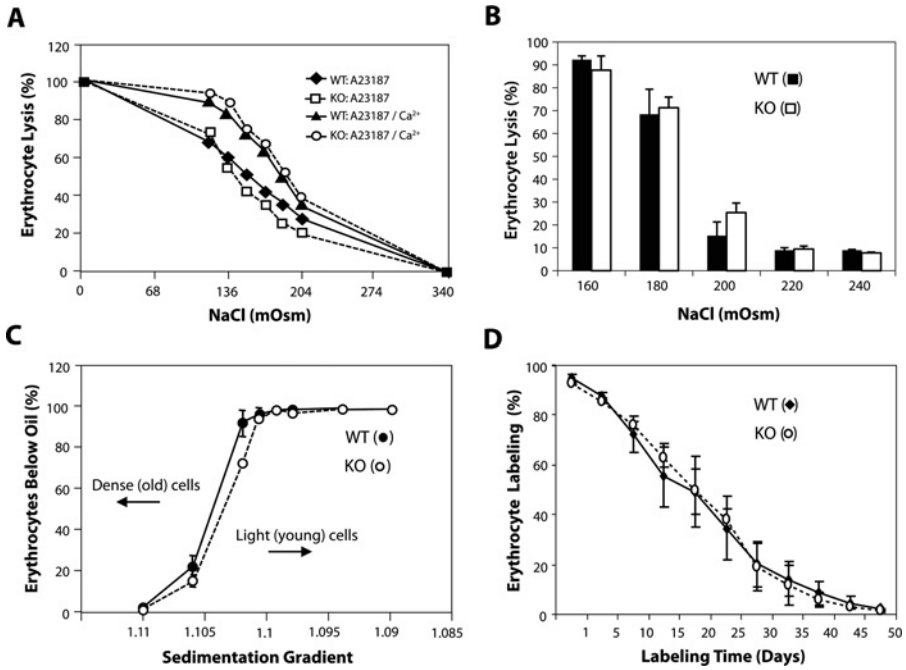

Figure 4 Erythrocyte osmotic fragility, density and lifespan measurements

(**A**) Washed erythrocytes from WT and calpain-1-null (KO) mice were subjected to the osmotic fragility test as described in the Experimental section. (**B**) Osmotic fragility of WT and KO erythrocytes was performed using a narrow range of salt concentrations. (**C**) Density gradient separation of light (young) and dense (old) erythrocytes from WT and KO mice. (**D**) Determination of erythrocyte lifespan *in vivo*. Flow cytometry was used to quantify the percentage of NHS–biotin-labelled erythrocytes as described in the Experimental section.

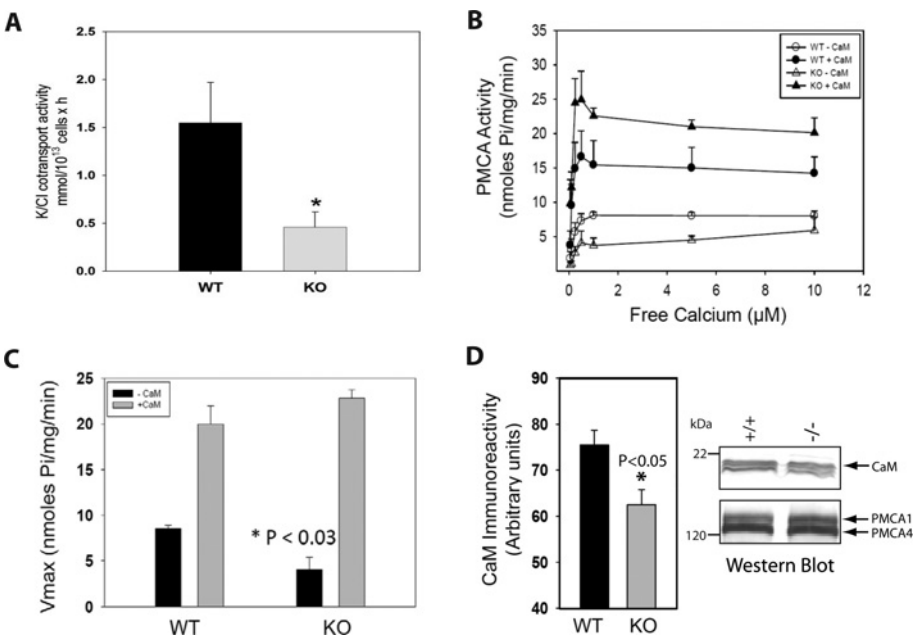

Figure 5 Measurement of KCC1 and calcium pump activity

(**A**) The K^+–Cl^- co-transport activity in the WT and calpain-1-null (KO) erythrocytes. The activity of KCC1 was measured as a volume-stimulated and Cl^--dependent component as described in the Experimental section ($P < 0.04$, $n = 3$). The values are expressed as mmol/10^{13} cells per h, and represent the means $\pm$ S.E.M. for three independent samples performed in triplicate. (**B**) Effect of increasing concentrations of free calcium on PMCA activity in the WT and KO ghosts in the absence and presence of 340 nM CaM ($n = 4$). (**C**) Calculated values of V_{max} of PMCA activity in the WT and KO ghosts ($n = 4$). (**D**) Immunoblot showing the level of CaM protein bound to WT and KO ghosts [50 μg of protein loaded on to SDS/PAGE (17% gel), 1:500 dilution of anti-CaM antibody, 1:1000 dilution of anti-mouse secondary antibody ($n = 3$)]. Densitometric analysis of the CaM immunoblot ($n = 3$). PMCA was used as a control for equal loading of the membrane proteins.

Table 1 AFM of mouse erythrocyte cytoskeleton

(i) WT erythrocytes

Parameter	No treatment			50 μM calcium		
Cytoskeleton height (nm)	7.06	6.96	6.75	7.89	7.72	7.65
Volume ($\times 10^6$) (nm^3)	5.14	5.62	5.36	5.27	5.25	5.64
Grain size ($\times 10^4$) (nm^2)	0.18	0.23	0.16	0.65	0.57	0.53

(ii) Calpain-1-null erythrocytes

Parameter	No treatment			50 μM calcium		
Cytoskeleton height (nm)	7.40	7.38	7.56	7.42	7.24	7.11
Volume ($\times 10^6$) (nm^3)	5.35	5.11	5.28	5.27	5.02	5.98
Grain size ($\times 10^4$) (nm^2)	0.29	0.45	0.41	0.39	0.34	0.48

quantified by Western blotting using an anti-CaM antibody in erythrocyte ghosts normalized by their PMCA content. The results from four independent experiments indicated a 17 % reduction in CaM bound to the calpain-1-null ghosts, a difference that was statistically significant ($P < 0.05$) (Figure 5D). Taken together, these results suggest that calpain-1 differentially regulates PMCA activity and CaM content in mouse erythrocyte membranes under these conditions.

AFM reveals a protective role of calpain-1 loss on erythrocyte membrane skeleton

AFM topographic images of WT erythrocyte membrane revealed an intact cytoskeleton network with fine filament structure (Figure 6) similar to the previously reported results [13,19,20]. Influx of 50 μM calcium in erythrocytes via calcium ionophore A23187 caused damage to the cytoskeleton integrity as evident by the absence of fine structure and elevated cytoskeleton height and grain size (Figure 6 and Table 1). AFM images of calcium-treated calpain-1-null erythrocytes also showed loss of fine structure, but the changes in the cytoskeleton height and grain size were much less pronounced than those observed in the calcium-treated WT controls (Figure 6 and Table 1). Consistent with the erythrocyte deformability data (Figure 3A), the loss of calpain-1 provided protection from the calcium-induced cytoskeleton instability as 50 μM calcium influx did not produce any significant change in the cytoskeleton height and grain size (Table 1). These results suggest that the loss of calpain-1 only slightly modifies the cytoskeletal network under steady-state conditions, and offers significant protection under conditions of calcium-induced calpain-1 activation in intact erythrocytes.

DISCUSSION

Since the discovery of the calpain system almost 50 years ago [30], the calcium-dependent neutral protease family has attracted considerable attention because of its involvement in numerous physiological processes [1,2,31]. There are 14 independent genes that encode calpain-related proteins; however, the term calpain activity generally refers to the cumulative activity of two calpains. Calpain-1 is activated at micromolar calcium concentrations, whereas calpain-2 is activated at millimolar calcium concentrations *in vitro*. Both calpains show overlapping substrate specificity, and are expressed in most mammalian cells. An exception is the adult erythrocyte, where the total calpain activity is contributed exclusively by calpain-1 [4]. Using calpain-1-null mice (KO) previously generated in our laboratory [4], in the present study we investigated the physiological function of calpain-1 in adult erythrocytes. Mature erythrocytes harvested from mice with a C57BL/6 genetic background were examined by casein zymography and Western blotting. As expected, no calpain polypeptide or activity was detected in the KO erythrocytes, consistent with our previous findings [4]. Thus generation of calpain-1-null mice with no gross haematological abnormality set the stage for interrogating the biological function of erythrocyte calpain-1 both *in vitro* and *in vivo*.

Our previous studies have shown that ankyrin, band 3, protein 4.1R, adducin and dematin are degraded in calcium-activated WT but not KO erythrocytes [23]. Similarly, the transglutaminase TG2 activity remained unaffected in calpain-1-null erythrocytes [23]. In the present study, the same set of erythrocyte membrane proteins was found to be resistant to calcium-induced degradation in calpain-1-null mice on a pure genetic background (Figure 1A). This finding is consistent with the previous identification of multiple substrates by direct binding of calpain to the erythrocyte membrane vesicles [32]. However, an unresolved issue remains with the identification of spectrin as a physiological substrate of calpain-1 in erythrocytes. For example, it has been shown that erythrocyte spectrin is degraded by calpain-1 *in vitro* [21,26]. In contrast, our results indicate that spectrin is not degraded in calcium-loaded erythrocytes either in the WT or KO mice (Figure 1). In our opinion, degradation of ankyrin that migrates under the spectrin band may account for this discrepancy. Alternatively, species differences, the concentration of calcium ionophores and incubation conditions are some of the other possibilities that could explain these apparently contradicting findings. Nonetheless, calpain-1 is likely to degrade non-erythroid spectrins, such as the brain fodrin, upon calcium activation. These models will now be testable in the calpain-1-null mice with a defined genetic background.

Several studies have shown that calpain-1 causes limited cleavage of PKC to generate PKM, whose biological function remains poorly defined [33,34]. One view supports the notion that limited proteolysis of PKC results in its constitutive activation, and the resultant PKM phosphorylates downstream targets in erythrocytes [8]. For example, treatment of erythrocytes with calpain inhibitors blocked PKC-mediated phosphorylation of protein 4.1R and protein 4.9 (dematin) with concomitant suppression of PKM [8]. An alternative model predicted that generation of PKM initiates the final degradation pathway of PKC, thus eventually depleting the enzyme [35]. Our results suggest that calpain-1 cleavage of PKC is not necessary for the phosphorylation of erythrocyte membrane proteins, irrespective of whether erythrocytes are stimulated by cAMP, PMA or calcium (Figure 1B). PKC serves as a substrate of calpain-1 since its degradation is inhibited in calpain-1-null erythrocytes activated by either calcium or PMA (Figure 1D). Moreover, phosphorylation of β-spectrin and other substrates remained unaltered despite partial degradation of PKC in normal erythrocytes (Figure 1B). These results suggest that spectrin degradation and phosphorylation are not regulated by calpain-1 in mouse erythrocytes under these conditions.

Previous evidence indicated a functional role of calpain-1 in the regulation of erythrocyte shape change [26]. Treatment of erythrocytes with a calpain inhibitor blocked their transition from echinocytes to spherocytes [26]. Similarly, purified cytoplasmic domain of band 3 is known to inhibit erythrocyte membrane shape change *in vitro* [36]. Our results from the present study indicate that calpain-1 functions as a key regulator of erythrocyte shape change (Figure 2). Moreover, our findings unveil some new aspects of erythrocyte shape regulation by calpain-1. The calpain-1 loss not only modulates the final erythrocyte shape change, but also affects the rate of shape transition in

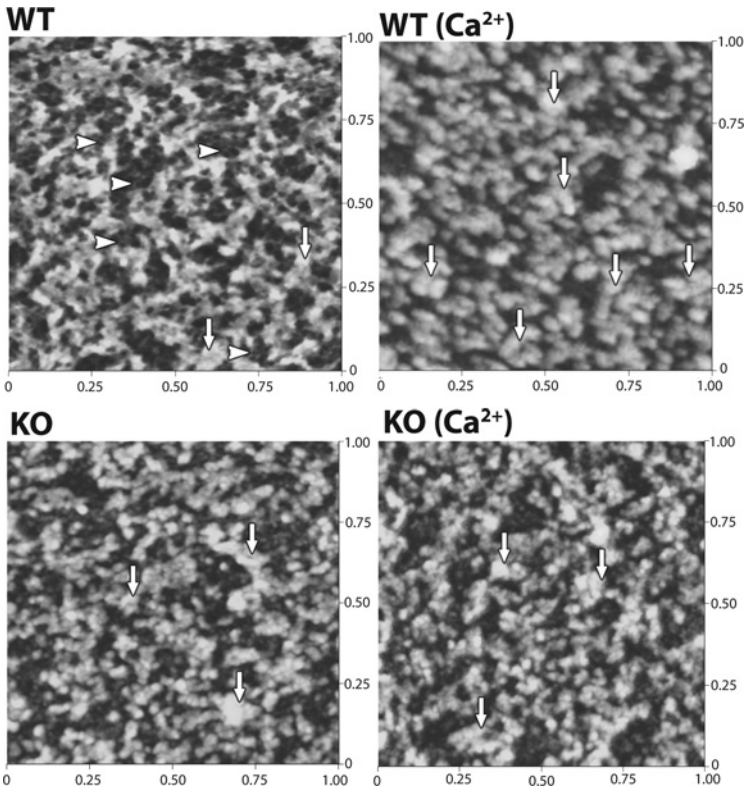

Figure 6 AFM of mouse erythrocyte skeleton

Washed erythrocytes in PBS were treated with calcium ionophore A23187 and 50 μM calcium, attached on to the glass coverslips, lysed to expose the intracellular surface of the cytoskeleton, and imaged using AFM essentially as described previously [13,19,20]. Images of WT erythrocyte cytoskeleton reveal an intact cytoskeleton network with fine filament structures similar to the results previously reported [13,19,20]. Treatment of WT erythrocytes with calcium resulted in the damage of the cytoskeleton integrity as evident by diminished fine structures and increased aggregates. AFM images of the calpain-1-null (KO) erythrocyte cytoskeleton show a similar loss of the fine structures (arrowheads) but fewer aggregates (arrows) were observed as compared with calcium-treated WT controls, suggesting that the calpain-1 loss may only slightly modify the cytoskeleton. No detectable structural changes were observed in the KO cytoskeleton upon calcium treatment of erythrocytes as compared with KO control cells, suggesting that calpain-1 loss protects erythrocytes from the calcium-induced cytoskeleton instability.

a calcium-dependent manner (Figure 2). In contrast with the previous study [26], the discocyte to echinocyte shape transition is potentiated in calpain-1 KO at a lower calcium concentration (Figure 2A). At higher calcium concentrations, the rate of discocyte–echinocyte transition was further augmented, thus rapidly generating the end-stage spherocytes (Figure 2B). These findings suggest that degradation of ankyrin, band 3, protein 4.1R and dematin by calpain-1 negatively regulates erythrocyte shape change, whereas spectrin degradation and phosphorylation are not necessary for this regulation under these conditions. Previously, we have shown that calpain-1 loss does not affect the phospholipid asymmetry, particularly erythrocyte surface exposure of phosphatidylserine [37]. Taken together, our findings offer an alternative model for the long-held view that the lipid bilayer serves as a dominant regulatory site for erythrocyte discocyte–echinocyte shape transition *in vivo* [38].

The shape and mechanical properties of erythrocytes are thought to be partially controlled by the submembrane network referred to as the membrane skeleton. Regulatory modifications of skeletal proteins, such as oxidation, proteolysis and phosphorylation have been known to influence the mechanical properties of erythrocytes by altering critical protein interactions. Because the calcium-induced phosphorylation of membrane proteins remains normal in calpain-1-null erythrocytes (Figure 1B), the KO model allowed us to directly evaluate the impact of moderate skeletal protein proteolysis on erythrocyte mechanical properties without complications arising from differences in protein phosphorylation. Our results provide the first evidence that inhibition of calcium-induced proteolysis of skeletal proteins in intact erythrocytes offers significant improvement in cell deformability and filtration rate (Figure 3). It is conceivable that one or more of the calpain-1 substrates in the erythrocyte membrane must remain intact to assure maximal deformability and filtration through pores smaller than the erythrocyte diameter.

The inhibition of erythrocyte skeletal protein degradation in calpain-1-null mice does not influence their lifespan *in vivo* under resting conditions (Figure 4D). Similarly, other haematological parameters, such as bilirubin, iron, haem and lactate dehydrogenase were unaffected in the KO mice (results not shown). The reticulocyte count was also normal in calpain-1-null mice. To reconcile subtle hydration phenotype in calpain-1-null erythrocytes (Figure 4B), we measured erythrocyte MCV (mean cell volume) in six adult mice of each genotype. A small but statistically significant increase in the MCV of KO erythrocyes was found (Table 2). Mechanistically, partial inhibition of the Gardos channel and KCC1 (Figure 5A), and an increase in the intracellular magnesium concentration (Table 2), could potentially contribute to modest MCV increase in KO erythrocytes, since these systems are known to play a functional role in erythrocyte volume regulation [16,39,40]. Alternatively, calpain-1 loss may trigger down-regulation of as yet unknown membrane-associated protein phosphatases, thus causing inhibition of the KCC1 [41,42]. Some of these models will be testable in the calpain-1-null mice described in the present study.

Table 2 Comparison of calpain-1-null with WT erythrocytes

Values are means + S.E.M. ($n = 6$). MCHC, mean corpuscular haemoglobin concentration. Total intracellular ion concentration, mmol/kg of haemoglobin.

Parameter	WT erythrocytes	Calpain-1-null erythrocytes	*P* value
MCV (fl)	47.20 ± 0.92	49.50 ± 0.48	0.0298
Haematocrit (%)	35.88 ± 1.56	42.90 ± 3.06	0.0390
Haemoglobin (g/dl)	11.28 ± 0.39	13.58 ± 0.89	0.0252
MCHC (%)	32.44 ± 0.43	31.80 ± 0.35	0.1398
$[Na^+]_i$	4.58 ± 0.11	3.48 ± 0.16	0.0002
$[K^+]_i$	123.80 ± 4.12	116.22 ± 5.01	0.1350
$[Mg^{2+}]_i$	8.05 ± 0.14	8.92 ± 0.21	0.0027

Calcium influx exerts pleiotropic effects on multiple pathways in erythrocytes, including membrane ion transport. One of the key determinants of intracellular calcium is the integral membrane protein referred to as calcium pump or PMCA [6,43,44]. The PMCA utilizes metabolic energy from ATP hydrolysis to transport Ca^{2+} across the plasma membrane against a 10000-fold gradient, thus playing a critical role in maintaining precise levels of intracellular calcium. The PMCA is a ~140 kDa protein with ten transmembrane helices and several intracellular domains, including its active site located between transmembrane segments 4 and 5. The C-terminal end of the PMCA contains an autoinhibitory domain, which interacts with its catalytic site, preventing the binding and utilization of ATP, thus keeping the enzyme in a state of low activity [45]. Binding of CaM, a calcium-binding protein, to PMCA triggers the dissociation of the autoinhibitory domain away from the catalytic core and release of autoinhibition, thus stimulating PMCA activity several-fold and providing the driving force for Ca^{2+} transport across the plasma membrane [45–48]. As shown in Figure 5, differential regulation of PMCA activity and CaM content in calpain-1-null erythrocytes may offer a potential mechanistic explanation for the regulation of erythrocyte cell shape, deformability, filterability and MCV. Since excessive calcium influx is a hallmark of several erythrocyte diseases, including sickle cell anaemia [39,49,50], our findings raise the possibility that pharmacological inhibition of calpain-1 may offer a therapeutic option against sickle cell disease and other calcium-related pathologies.

AUTHOR CONTRIBUTION

Adam Wieschhaus performed microscopy and other experiments, analysed the data and wrote sections of the paper. Anwar Khan performed *in vivo* lifespan and other experiments and wrote a section of the paper. Asma Zaidi performed calcium pump measurements and wrote a section of the paper. Henry Rogalin performed deformability experiments and wrote a section of the paper. Toshihiko Hanada typed mutant mice, supervised several experiments and edited the paper. Fei Liu performed AFM experiments and wrote a section of the paper. Lucia De Franceschi gave technical advice and edited the paper. Carlo Brugnara and Alicia Rivera performed erythrocyte transport assays and wrote sections of the paper. Athar Chishti performed calcium loading and *in vivo* phosphorylation experiments, designed the study, analysed the data and wrote the paper.

ACKNOWLEDGEMENTS

We thank Seon Hee Chang and Philip Low of Purdue University for performing the erythrocyte filterability measurements, and Agnes Ostafin of the University of Notre Dame where some of the AFM experiments were performed. We are also grateful to C.S. Hong of Rheomeditech for loaning us their Rheoscan D-300 Ektacytometer to complete the erythrocyte deformability measurements. We greatly appreciate the contributions of Ronald Dubreuil, Mohammad Azam, Richie Khanna, Katrin Kiessling, Shafi Kuchay and Gerald O'Neill at various stages of this study. Finally, we thank Donna-Marie Mironchuk for assistance with the artwork and careful proofreading of the paper prior to submission.

FUNDING

This work was supported by the National Institutes of Health [grant numbers HL089517 and HL095050 (to A.H.C.) and HL090632 (to A.R.)].

REFERENCES

1 Goll, D. E., Thompson, V. F., Li, H., Wei, W. and Cong, J. (2003) The calpain system. Physiol. Rev. **83**, 731–801
2 Yamada, K. H., Kozlowski, D. A., Seidl, S. E., Lance, S., Wieschhaus, A. J., Sundivakkam, P., Tiruppathi, C., Chishti, I., Herman, I. M., Kuchay, S. M. and Chishti, A. H. (2012) Targeted gene inactivation of calpain-1 suppresses cortical degeneration due to traumatic brain injury and neuronal apoptosis induced by oxidative stress. J. Biol. Chem. **287**, 13182–13193
3 Kawasaki, H. and Kawashima, S. (1996) Regulation of the calpain-calpastatin system by membranes (review). Mol. Membr. Biol. **13**, 217–224
4 Azam, M., Andrabi, S. S., Sahr, K. E., Kamath, L., Kuliopulos, A. and Chishti, A. H. (2001) Disruption of the mouse μ-calpain gene reveals an essential role in platelet function. Mol. Cell. Biol. **21**, 2213–2220
5 Carafoli, E. (1991) Calcium pump of the plasma membrane. Physiol. Rev. **71**, 129–153
6 Strehler, E. E. and Zacharias, D. A. (2001) Role of alternative splicing in generating isoform diversity among plasma membrane calcium pumps. Physiol. Rev. **81**, 21–50
7 Hayashi, M., Saito, Y. and Kawashima, S. (1992) Calpain activation is essential for membrane fusion of erythrocytes in the presence of exogenous Ca^{2+}. Biochem. Biophys. Res. Commun. **182**, 939–946
8 Al, Z. and Cohen, C. M. (1993) Phorbol 12-myristate 13-acetate-stimulated phosphorylation of erythrocyte membrane skeletal proteins is blocked by calpain inhibitors: possible role of protein kinase M. Biochem. J. **296**, 675–683
9 Schoenwaelder, S. M. and Burridge, K. (1999) Evidence for a calpeptin-sensitive protein-tyrosine phosphatase upstream of the small GTPase Rho. A novel role for the calpain inhibitor calpeptin in the inhibition of protein-tyrosine phosphatases. J. Biol. Chem. **274**, 14359–14367
10 Baskurt, O. K., Hardeman, M. R., Uyuklu, M., Ulker, P., Cengiz, M., Nemeth, N., Shin, S., Alexy, T. and Meiselman, H. J. (2009) Comparison of three commercially available ektacytometers with different shearing geometries. Biorheology **46**, 251–264
11 Shin, S., Hou, J. X., Suh, J. S. and Singh, M. (2007) Validation and application of a microfluidic ektacytometer (RheoScan-D) in measuring erythrocyte deformability. Clin. Hemorheol. Microcirc. **37**, 319–328
12 Arai, K., Iino, M., Shio, H. and Uyesaka, N. (1990) Further investigations of red cell deformability with nickel mesh. Biorheology **27**, 47–65
13 Chen, H., Khan, A. A., Liu, F., Gilligan, D. M., Peters, L. L., Messick, J., Haschek-Hock, W. M., Li, X., Ostafin, A. E. and Chishti, A. H. (2007) Combined deletion of mouse dematin-headpiece and β-adducin exerts a novel effect on the spectrin-actin junctions leading to erythrocyte fragility and hemolytic anemia. J. Biol. Chem. **282**, 4124–4135
14 White, J. G. (1974) Effects of an ionophore, A23187, on the surface morphology of normal erythrocytes. Am. J. Pathol. **77**, 507–518
15 Rivera, A., Rotter, M. A. and Brugnara, C. (1999) Endothelins activate Ca^{2+}-gated K^+ channels via endothelin B receptors in CD-1 mouse erythrocytes. Am. J. Physiol. **277**, C746–C754
16 Bize, I., Taher, S. and Brugnara, C. (2003) Regulation of K-Cl cotransport during reticulocyte maturation and erythrocyte aging in normal and sickle erythrocytes. Am. J. Physiol. Cell Physiol. **285**, C31–C38
17 Zaidi, A., Leclerc-L'Hostis, E., Marden, M. C., Poyart, C. and Leclerc, L. (1995) Heme as an optical probe for studying the interactions between calmodulin and the Ca^{2+}-ATPase of the human erythrocyte membrane. Biochim. Biophys. Acta **1236**, 114–118
18 Zaidi, A., Fernandes, D., Bean, J. L. and Michaelis, M. L. (2009) Effects of paraquat-induced oxidative stress on the neuronal plasma membrane Ca^{2+}-ATPase. Free Radical Biol. Med. **47**, 1507–1514
19 Liu, F., Burgess, J., Mizukami, H. and Ostafin, A. (2003) Sample preparation and imaging of erythrocyte cytoskeleton with the atomic force microscopy. Cell Biochem. Biophys. **38**, 251–270
20 Liu, F., Khan, A. A., Chishti, A. H. and Ostafin, A. E. (2011) Atomic force microscopy demonstration of cytoskeleton instability in mouse erythrocytes with dematin-headpiece and β-adducin deficiency. Scanning **33**, 426–436
21 Boivin, P., Galand, C. and Dhermy, D. (1990) *In vitro* digestion of spectrin, protein 4.1 and ankyrin by erythrocyte calcium dependent neutral protease (calpain I). Int. J. Biochem. **22**, 1479–1489
22 Hatanaka, M., Yoshimura, N., Murakami, T., Kannagi, R. and Murachi, T. (1984) Evidence for membrane-associated calpain I in human erythrocytes. Detection by an immunoelectrophoretic blotting method using monospecific antibody. Biochemistry **23**, 3272–3276

23 O'Neill, G. M., Prasanna Murthy, S. N., Lorand, L., Khanna, R., Liu, S. C., Hanspal, M., Hanada, T. and Chishti, A. H. (2003) Activation of transglutaminase in μ-calpain null erythrocytes. Biochem. Biophys. Res. Commun. **307**, 327–331

24 Cohen, C. M. and Gascard, P. (1992) Regulation and post-translational modification of erythrocyte membrane and membrane-skeletal proteins. Semin. Hematol. **29**, 244–292

25 Pontremoli, S., Michetti, M., Melloni, E., Sparatore, B., Salamino, F. and Horecker, B. L. (1990) Identification of the proteolytically activated form of protein kinase C in stimulated human neutrophils. Proc. Natl. Acad. Sci. U.S.A. **87**, 3705–3707

26 Hayashi, M., Inomata, M., Saito, Y., Ito, H. and Kawashima, S. (1991) Activation of intracellular calcium-activated neutral proteinase in erythrocytes and its inhibition by exogenously added inhibitors. Biochim. Biophys. Acta **1094**, 249–256

27 Jakubowska-Solarska, B. and Solski, J. (2000) Sialic acids of young and old red blood cells in healthy subjects. Med. Sci. Monit. **6**, 871–874

28 Jarrett, H. W. and Penniston, J. T. (1977) Partial purification of the Ca^{2+}-Mg^{2+} ATPase activator from human erythrocytes: its similarity to the activator of 3′:5′-cyclic nucleotide phosphodiesterase. Biochem. Biophys. Res. Commun. **77**, 1210–1216

29 Zaidi, A. and Michaelis, M. L. (1999) Effects of reactive oxygen species on brain synaptic plasma membrane Ca^{2+}-ATPase. Free Radical Biol. Med. **27**, 810–821

30 Guroff, G. (1964) A neutral calcium-activated proteinases from the soluble fraction of rat brain. J. Biol. Chem. **239**, 149–155

31 Kuchay, S. M., Wieschhaus, A. J., Marinkovic, M., Herman, I. M. and Chishti, A. H. (2012) Targeted gene inactivation reveals a functional role of calpain-1 in platelet spreading. J. Thromb. Haemost. **10**, 1120–1132

32 Kuboki, M., Ishii, H. and Kazama, M. (1990) Characterization of calpain I-binding proteins in human erythrocyte plasma membrane. J. Biochem. **107**, 776–780

33 Kishimoto, A., Mikawa, K., Hashimoto, K., Yasuda, I., Tanaka, S., Tominaga, M., Kuroda, T. and Nishizuka, Y. (1989) Limited proteolysis of protein kinase C subspecies by calcium-dependent neutral protease (calpain). J. Biol. Chem. **264**, 4088–4092

34 Parker, P. J., Coussens, L., Totty, N., Rhee, L., Young, S., Chen, E., Stabel, S., Waterfield, M. D. and Ullrich, A. (1986) The complete primary structure of protein kinase C–the major phorbol ester receptor. Science **233**, 853–859

35 Kishimoto, A., Kajikawa, N., Shiota, M. and Nishizuka, Y. (1983) Proteolytic activation of calcium-activated, phospholipid-dependent protein kinase by calcium-dependent neutral protease. J. Biol. Chem. **258**, 1156–1164

36 Carter, D. P. and Fairbanks, G. (1984) Inhibition of erythrocyte membrane shape change by band 3 cytoplasmic fragment. J. Cell. Biochem. **24**, 385–393

37 Sarang, Z., Madi, A., Koy, C., Varga, S., Glocker, M. O., Ucker, D. S., Kuchay, S., Chishti, A. H., Melino, G., Fesus, L. and Szondy, Z. (2007) Tissue transglutaminase (TG2) facilitates phosphatidylserine exposure and calpain activity in calcium-induced death of erythrocytes. Cell Death Differ. **14**, 1842–1844

38 Daleke, D. L. and Huestis, W. H. (1989) Erythrocyte morphology reflects the transbilayer distribution of incorporated phospholipids. J. Cell Biol. **108**, 1375–1385

39 Brugnara, C., Bunn, H. F. and Tosteson, D. C. (1986) Regulation of erythrocyte cation and water content in sickle cell anemia. Science **232**, 388–390

40 Rivera, A., Ferreira, A., Bertoni, D., Romero, J. R. and Brugnara, C. (2005) Abnormal regulation of Mg^{2+} transport via Na/Mg exchanger in sickle erythrocytes. Blood **105**, 382–386

41 Bize, I., Guvenc, B., Buchbinder, G. and Brugnara, C. (2000) Stimulation of human erythrocyte K-Cl cotransport and protein phosphatase type 2A by n-ethylmaleimide: role of intracellular Mg^{++}. J. Membr. Biol. **177**, 159–168

42 Bize, I., Guvenc, B., Robb, A., Buchbinder, G. and Brugnara, C. (1999) Serine/threonine protein phosphatases and regulation of K-Cl cotransport in human erythrocytes. Am. J. Physiol. **277**, C926–C936

43 Carafoli, E. (1992) The Ca^{2+} pump of the plasma membrane. J. Biol. Chem. **267**, 2115–2118

44 Brini, M. and Carafoli, E. (2009) Calcium pumps in health and disease. Physiol. Rev. **89**, 1341–1378

45 Falchetto, R., Vorherr, T. and Carafoli, E. (1992) The calmodulin-binding site of the plasma membrane Ca^{2+} pump interacts with the transduction domain of the enzyme. Protein Sci. **1**, 1613–1621

46 Enyedi, A., Vorherr, T., James, P., McCormick, D. J., Filoteo, A. G., Carafoli, E. and Penniston, J. T. (1989) The calmodulin binding domain of the plasma membrane Ca^{2+} pump interacts both with calmodulin and with another part of the pump. J. Biol. Chem. **264**, 12313–12321

47 James, P., Maeda, M., Fischer, R., Verma, A. K., Krebs, J., Penniston, J. T. and Carafoli, E. (1988) Identification and primary structure of a calmodulin binding domain of the Ca^{2+} pump of human erythrocytes. J. Biol. Chem. **263**, 2905–2910

48 Johnson, C. K., Liyanage, M. R., Osborn, K. D. and Zaidi, A. (2011) Single-protein dynamics and the regulation of the plasma-membrane Ca^{2+} pump. Cell Signaling Reactions **2011**, 121–151

49 Liu, S. C., Derick, L. H., Zhai, S. and Palek, J. (1991) Uncoupling of the spectrin-based skeleton from the lipid bilayer in sickled red cells. Science **252**, 574–576

50 Palek, J., Thomae, M. and Ozog, D. (1977) Red cell calcium content and transmembrane calcium movements in sickle cell anemia. J. Lab. Clin. Med. **89**, 1365–1374

Received 21 June 2012/3 August 2012; accepted 8 August 2012
Published as BJ Immediate Publication 8 August 2012, doi:10.1042/BJ20121008